Thermoelectric power and electrical resistance of thin, quench-condensed Sb/Au bilayers - a study of an amorphous phase at the interface

1996 J. Phys.: Condens. Matter 8 6653

(http://iopscience.iop.org/0953-8984/8/36/017)

J. Phys.: Condens. Matter **8** (1996) 6653–6663. Printed in the UK

Thermoelectric power and electrical resistance of thin, quench-condensed Sb/Au bilayers—a study of an amorphous phase at the interface

C Lauinger†§, F Baumann† and H-G Boyen‡

† Physikalisches Institut, Universität Karlsruhe, 76128 Karlsruhe, Germany

‡ Institut für Physik, Universität Basel, Klingelbergstraße 82, 4056 Basel, Switzerland

Received 10 April 1996, in final form 19 June 1996

Abstract. Our investigation of the electrical resistance and the thermoelectric power of thin Au films on top of amorphous Sb films as a function of increasing thickness of the Au film allows us to compare the data with those on amorphous Au_xSb_{100-x} films with increasing Au content. The comparison shows a substantial similarity of the low-temperature data as well as of the annealing behaviour. This gives additional support to the hypothesis of the formation of an amorphous phase at the interface in layered Sb/Au films. The thicknesses of those parts of the Sb film and the Au film which contribute to the formation of the amorphous interface are determined and agree well with data taken from photoelectron spectroscopy and resistance measurements during evaporation. The quantitative differences which exist in the concentration dependence of the electrical resistance and the thermoelectric power between the Sb/Au bilayers and the amorphous Au_xSb_{100-x} films are probably caused by the reduced geometry of the ultrathin interface.

1. Introduction

The physical and chemical interaction between different films deposited on top of each other has been subject to many investigations in solid-state physics. The increasing interaction between different elements during the early stage of formation of multilayers has been studied intensively by *in situ* investigations as a function of film thicknesses [1, 2, 3, 4, 5]. In order to keep the diffusion as small as possible one has either to concentrate on elements which are highly insoluble or to carry out the measurements for the as-quenched state at low temperatures.

Photoelectron spectroscopy on Sb/Au bilayers as well as electrical resistance measurements during the evaporation of Sb/Au multilayers clearly demonstrate the formation of an amorphous phase at the interface on a monolayer scale [6]. This amorphous phase can exist up to the thickness $d_{\mathrm{Au,max}}$ of the Au film on top of a thick Sb film while above this limit the Au film grows in a crystalline phase.

Pure Sb vapour quenched at low temperatures grows in a metastable amorphous phase which is semiconducting and which crystallizes into the thermodynamically stable phase during annealing at about 280 K [7, 8, 9]. Vapour-quenched pure Au films grow always in the stable crystalline phase. Vapour-quenched Au_xSb_{100-x} films with $x < 80$ at.% are homogeneously amorphous while films with $x > 80$ at.% are partly polycrystalline [10].

§ Present address: Institut für Physik, TU Chemnitz–Zwickau, 09107 Chemnitz, Germany.

0953-8984/96/366653+11$19.50

At $x_c = 8.1$ at.% these films show a metal–insulator transition [11]. Homogeneously amorphous films are metallic for $x_c < x < 80$ at.% and show superconductivity with a maximum $T_c \approx 3$ K at $x \approx 40$ at.% [10].

The crystallization temperature T_x of the alloys depends on the Au content and it is reduced from 280 K for pure Sb to 200 K at $x = 20$ at.%. With increasing Au content T_x also increases to 280 K at $x = 60$ at.% and this value remains constant for a further increase of x in the amorphous phase.

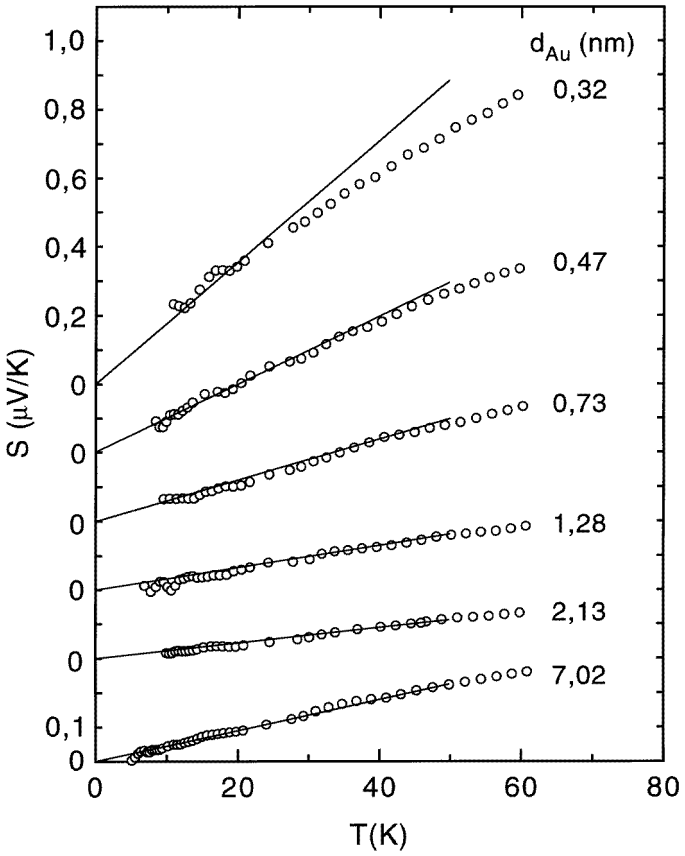

Figure 1. Thermopower of Sb/Au bilayers as a function of temperature measured after annealing at 60 K for different thicknesses d_{Au} of Au coverages on top of the Sb film. The data are linearly extrapolated to zero temperature.

Bilayers with a very low Au coverage are in an insulating state. Although this state is certainly worth studying it is not subject of this investigation. We focus our interest onto the metallic region up to $d_{Au,max}$ mentioned earlier. As known from photoelectron spectroscopy [6] and as will be shown in this investigation, Sb/Au bilayers behave as a function of increasing d_{Au} very similarly to amorphous Au_xSb_{100-x} alloys as a function of increasing x.

Thermoelectric power seems to us not only a sensitive quantity to use in order to characterize a material but also an ideal tool for investigating ultrathin films. The thermoelectric power of a three-dimensional sample does not depend on its size. In other

words, any change of the thermoelectric power of a film with decreasing thickness reflects directly the change of its properties. Measuring for example the electrical resistance of a film, the situation is different. The resistance reflects not only any change in the properties of the material but also changes in the thickness of the film or its area.

The purpose of this investigation is twofold. One reason is to give additional support to the formation of an amorphous phase at the interface in layered Sb/Au films. For this we compare our results with those of recent measurements of the thermoelectric power and the electrical resistivity of amorphous Au_xSb_{100-x} alloys [11]. This comparison shows qualitatively a large similarity between the three-dimensional Au_xSb_{100-x} alloys and the quasi-two-dimensional Sb/Au bilayers but it shows at the same time differences which in our opinion are probably caused by the restricted geometry. This is the second reason that we followed up during this investigation.

2. Some experimental details

The *in situ* measurements of the thermopower S and the electrical resistance per square $R_\square$ were performed in a ^{4}He cryostat. The thermopower was measured using a dynamical method in the temperature range between 5 K and 350 K. The resistance $R_\square$ was measured above 1.7 K using a standard four-wire DC technique. Further experimental details are given elsewhere [11, 13].

The Sb/Au double layers were prepared in a two-step evaporation process. At first a Sb film was evaporated onto the glass substrate which then was covered with a Au film of thickness d_{Au}. The thickness of the Sb films was held constant at approximately 12 nm, whereas d_{Au} varies between 0.3 nm and 7 nm. The evaporation rate of the Au increases from approximately 5×10^{-3} nm s^{-1} for the smallest Au coverage to 5×10^{-2} nm s^{-1} for the highest Au coverage. The thicknesses of the films were determined using a sensitive quartz oscillator assuming the density of the films to be equal to the bulk densities of the crystalline elements. During evaporation the pressure in the cryostat rose from about 3×10^{-8} mbar to approximately 5×10^{-7} mbar and at the same time the temperature of the sample holder increased to about 20 K. After the condensation process the samples were annealed step by step up to a temperature of 350 K. Besides the reversible temperature dependence of $S(T)$ and $R_\square(T)$ we also measured both quantities during annealing. In this paper we report the low-temperature data measured after a first annealing at 60 K and, in addition, some data measured during annealing.

3. Results

3.1. Thermoelectric power

The low-temperature data on the thermoelectric power $S(T)$ of the Sb/Au bilayers as well as their annealing behaviour are very much the same as those of amorphous Au_xSb_{100-x} alloys while they differ strongly from $S(T)$ for either polycrystalline Au films or amorphous Sb films [14].

Figure 1 shows the temperature dependence of the thermoelectric power $S(T)$ of Sb/Au bilayers. Although annealing effects below 60 K are negligible, all of the samples are annealed at 60 K immediately after condensation. Apparently all bilayers show at low temperatures a linear increase of S with temperature. The results are summarized in figure 2 where the slope of $S(T)$ extrapolated to zero temperature is shown as a function of d_{Au}. In addition data taken from polycrystalline Au films quenched directly onto a glass substrate are

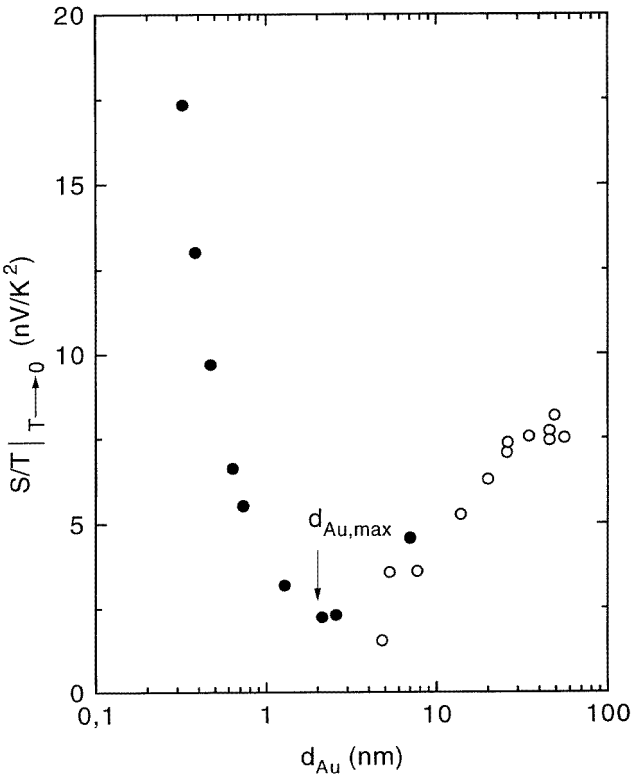

Figure 2. The low-temperature slopes of the thermopower of Sb/Au bilayers (•) and of pure polycrystalline Au films (○) as functions of the Au thickness.

also shown. $S(T)$ for these films is proportional to the temperature as long as $T < 60$ K. The slope S/T is constant in the region where $d_{\mathrm{Au}} > 30$ nm whereas it decreases with decreasing d_{Au} at low Au thicknesses. The thickness dependence of S/T for crystalline films is difficult to analyse, as outlined in reference [15]. It has been shown that voids, channels, and rough surfaces may dominate the thickness dependence of $S(T)$ in thin films. However, for a quantitative analysis of the data, the topological structure of the films as well as other parameters which describe the scattering of the electrons have to be known. Therefore at the moment a more detailed analysis of the data does not seem possible. However, it is interesting to note that S/T decreases in a region where the low-temperature value of $R_{\square}$ increases rapidly (see figure 3 below) when approaching the percolation transition, which is reached at $d_{\mathrm{Au}} \approx 4$–5 nm. Au films with smaller thicknesses are discontinuous and measurements of the thermopower are therefore not possible.

In the case of the bilayers, $S/T|_{T\to 0}$ shows above $d_{\mathrm{Au}} \approx 2$ nm the same behaviour as polycrystalline Au films. However, below $d_{\mathrm{Au}} \approx 2$ nm a drastic increase of $S/T|_{T\to 0}$ with decreasing Au coverage is observed. At first sight the behaviour of the Sb/Au bilayers shown in figure 2 seems very similar to the concentration dependence of the low-temperature slope of $S(T)$ for amorphous $\mathrm{Au}_x\mathrm{Sb}_{100-x}$ alloys which can be seen in figure 6 of reference [11]. In both cases there is a drastic decrease in $S/T|_{T\to 0}$ which is followed by a small minimum with increasing x or d_{Au}. However, a quantitative discussion given later shows distinct differences.

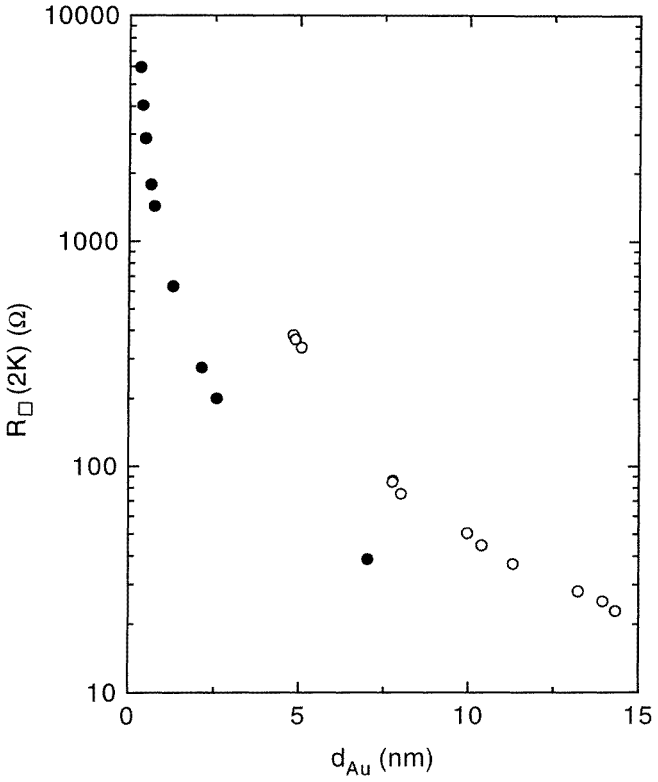

Figure 3. Resistances per square $R_\square$(2 K) of Sb/Au bilayers (•) and polycrystalline Au films (○) as functions of the Au thickness. The bilayers were annealed at 60 K and the pure Au films at 25 K.

3.2. Electrical resistance

Figure 3 shows the resistance per square at 2 K, i.e. $R_\square$(2 K), for Sb/Au bilayers as a function of the thickness d_{Au} of the Au top layer. In addition, data on pure Au films directly quenched onto a glass substrate are also shown. The bilayers as well as the pure Au films show a strong increase in $R_\square$(2 K) with decreasing d_{Au}. This increase signals in both cases the transition from the metallic phase to an insulator. Quenched pure Au films reach the percolation limit at about $d_{Au} \approx 4$–5 nm. Thinner Au films are discontinuous. In the case of the bilayers the transition occurs at a much smaller Au coverage, i.e. $d_{Au} \approx 0.2$–0.3 nm.

It should be mentioned that superconducting fluctuations above the transition temperature have been observed in bilayers in the thickness range 0.8 nm $< d_{Au} <$ 2–3 nm. This indicates that a chemical interaction has taken place at the interface because the elements in their pure form are not superconducting in contrast to amorphous Au_xSb_{100-x} alloys and metastable Au_xSb_{100-x} mixed crystals. While the amorphous Au_xSb_{100-x} alloys [11] and the metastable Au_xSb_{100-x} mixed crystals [16] have a maximum $T_c \approx 3$ K at $x = 40$ at.% and a maximum $T_c \approx 6.8$ K at $x = 22$ at.%, the transition temperatures of the bilayers are shifted to temperatures below 1.5 K which is the lower-temperature limit of the ^{4}He cryostat. This shift is expected because of the proximity effect and the small thickness of the top layer. We suppose that the superconducting fluctuations in the bilayers indicate

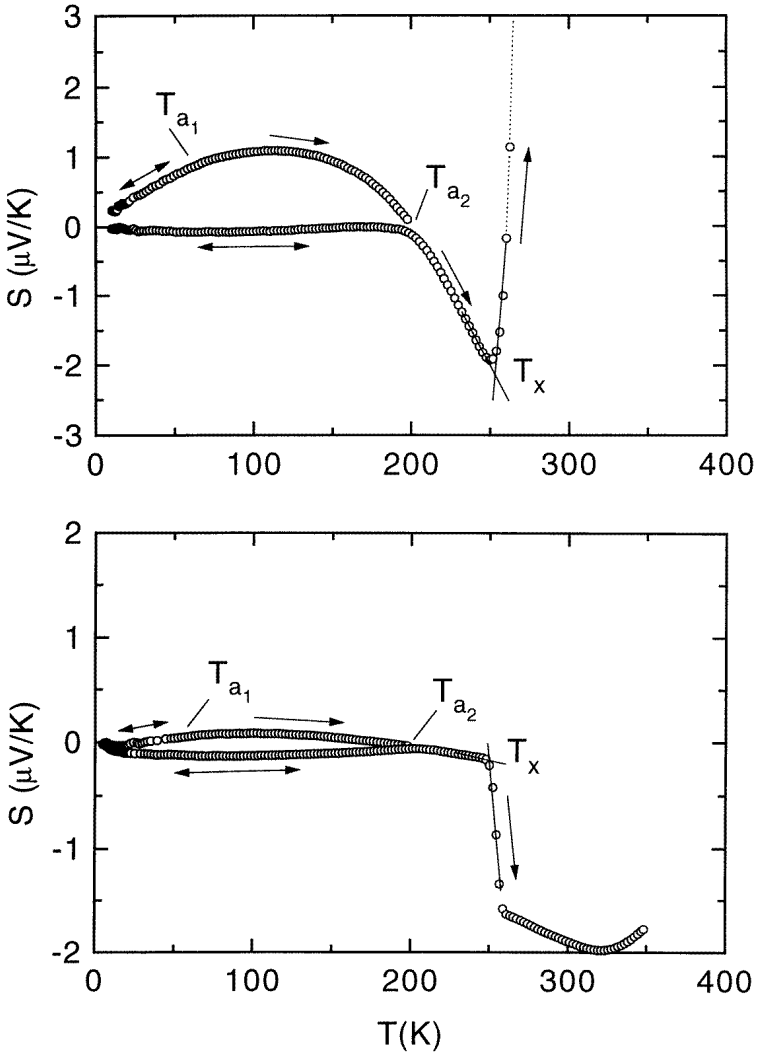

Figure 4. Annealing behaviour of $S(T)$ for a Sb/Au bilayer with $d_{\mathrm{Au}} = 0.32$ nm (upper part) and of an amorphous $Au_{37}Sb_{63}$ film (lower part). Arrows indicate irreversible ($\longrightarrow$) and reversible ($\longleftrightarrow$) changes. T_{a_1} and T_{a_2} are the annealing temperatures in the amorphous state. T_x is the crystallization temperature.

the occurrence of the amorphous Au_xSb_{100-x} phase and not the presence of a metastable mixed crystal, which in quench-condensed films is not formed completely before the films are annealed to at least 200 K [16].

3.3. Annealing behaviour

While annealing of the bilayers below 60 K has nearly no effect on $S(T)$ and $R_{\square}(T)$, distinct irreversible changes occur at higher temperatures. As an example the behaviour of a Sb/Au bilayer with $d_{\mathrm{Au}} = 0.32$ nm will be shown in the following. As discussed later

there are arguments that this bilayer corresponds to an alloy with $x \approx 40$ at.%. Therefore the annealing behaviour of $S(T)$ and $R_{\square}(T)$ for the bilayer will be compared with that for an amorphous $Au_{37}Sb_{63}$ alloy.

In figure 4 the annealing behaviour of $S(T)$ for both samples is shown. In both cases there is a maximum in $S(T)$ at about 100 K observed during annealing. The height of the maximum however is much more pronounced in the case of the bilayer. Such a maximum is a characteristic feature for bilayers with Au coverages smaller than approximately 0.6–0.7 nm whereas in the case of the amorphous alloys it appears for $x < 20$ at.% and $x \approx 40$ at.%. The reversible data taken after annealing to about 200 K are for both samples very much the same—as is the crystallization temperature which is $T_x \approx 260$ K. It is not surprising that after the crystallization $S(T)$ for both samples differs, because in this case the total Sb film of the bilayer comes suddenly into play.

In figure 5 the annealing behaviour of the electrical resistance is shown. Both samples show a reversible negative temperature coefficient of $R_{\square}$ or ρ after recooling as long as the annealing temperature is below T_x. In both cases the electrical resistance is irreversibly decreasing due to annealing. However, this behaviour is much more pronounced in the case of the bilayer. This may be caused by small changes of the geometry of the ultrathin film during annealing. It is worth noticing that the crystallization process in the bilayer shown in the last two figures takes place within a small temperature region. This behaviour is known from metastable alloys as long as they are homogeneous. We take the sudden decrease at T_x in the figures mentioned as an additional hint in favour of homogeneity of the amorphous interface.

4. Discussion

The comparison between the transport properties of Sb/Au bilayers and amorphous Au_xSb_{100-x} alloys presented in the last section showed qualitatively an astonishing similarity in the properties under investigation. This is true not only of the annealed state but also during annealing.

We will discuss our results with the help of an amorphous interface model. In the model the interface is built up by the Au film of thickness d_{Au} and an underlying effective Sb film of thickness $d_{Sb,eff}$ and is described as a homogeneous amorphous alloy of thickness $d = d_{Au} + d_{Sb,eff}$. The model is based on photoelectrical investigations (UPS, XPS) of Sb/Au [6] and mainly of Sn/Au bilayers and the corresponding amorphous alloy [17]. Firstly, UPS measurements as a function of d_{Au} and x, respectively, showed identical sequences of spectra for the bilayers and the amorphous films. This allows us to determine the Au concentration x of the interface as a function of the Au overlayer thickness using the binding energy of the Au $5d_{5/2}$ band. On the basis of this concentration scale, strong binding energy shifts are found in XPS core-level spectra for the Au 4f lines, which are identical in the interface layers and the corresponding amorphous films. Most importantly, the widths of the narrow Au 4f core lines are also identical in the bilayers and the alloy films. In the case of a concentration gradient in the interface layer one would expect a significantly increased line width compared with that of the corresponding homogeneous amorphous film. The latter result gives strong support to the assumption of a homogeneous amorphous interface made in the model.

Because of the insulating behaviour of amorphous pure Sb it is possible to measure directly the electrical transport properties of the amorphous interface. Neither in the electrical resistance nor in the thermoelectric power does the amorphous Sb film of the bilayer come fully into play. Only that part of the Sb film with thickness $d_{Sb,eff}$ in contact

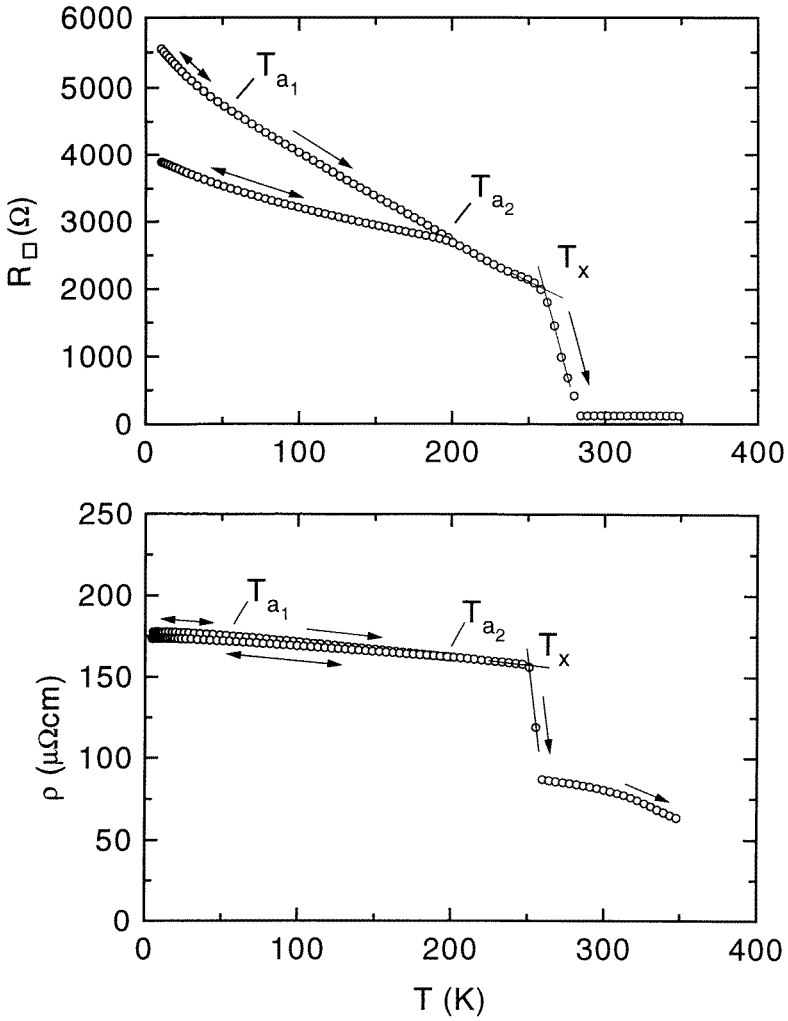

Figure 5. Annealing behaviour of $R_\square(T)$ for a Sb/Au bilayer with $d_{\mathrm{Au}} = 0.32$ nm (upper part) and of $\rho(T)$ for an amorphous $Au_{37}Sb_{63}$ film (lower part). Arrows indicate irreversible ($\longrightarrow$) and reversible ($\leftarrow\rightarrow$) changes. T_{a_1} and T_{a_2} are the annealing temperatures in the amorphous state. T_x is the crystallization temperature.

with the Au film contributes to the electrical properties of the bilayer. Most of the amorphous Sb film serves simply as a substrate for the interface.

The thermopower data allow us to determine $d_{\mathrm{Au,max}} = 2$ nm from the position of the minimum in figure 2 marked by an arrow. Bilayers with thicker Au coverages are partly crystalline. Supposing that in the bilayer with $d_{\mathrm{Au,max}} = 2$ nm (corresponding to 7.5 ML) an amorphous interface with an average Au content of 80 at.% is formed, then the effective Sb layer is $d_{\mathrm{Sb,eff}} = 0.8$ nm (corresponding to 2.6 ML).

The values just mentioned can be compared with data taken from the literature. Boyen *et al* [6] measured the electrical resistance of Sb/Au multilayers during the evaporation process at a substrate temperature of 130 K. In the case of a Au/Sb bilayer the resistance

decreases during the evaporation of the Au film (4.2 nm) but increases and finally saturates as the Sb film (15 nm) is evaporated on top of the Au film. The authors interpret the increase of the resistance as being caused by the formation of an amorphous Au_xSb_{100-x} interface which has a higher resistivity than polycrystalline Au. During the evaporation of a Au film on top of amorphous Sb the resistance decreases at first slowly (up to about 1.5 nm) and finally much faster although the evaporation rate was held constant. These experiments give $d_{Au,max} \approx 1.5$ nm together with $d_{Sb,eff} \approx 1$ nm.

Boyen *et al* observed in their investigation also the onset of crystallization on top of a Sb/Au bilayer by UPS and XPS measurements [6]. As in the case of Au_xSb_{100-x} for $x \geqslant 80$ at.% the onset of the growing of crystalline Au on top of the Sb/Au bilayers can be seen from the occurrence of additional structures in the UPS spectra which are typical for crystalline films. From these measurements the maximum Au coverage without any crystalline parts is $d_{Au,max} \approx 1.5$ nm. Under the assumption that in this upper limit the average Au content of the amorphous interface is $x = 80$ at.% the thickness $d_{Sb,eff} \approx 0.8$ nm. Hence the values given by Boyen *et al* agree well with the values given in the present paper.

So far we have discussed the upper limit $d_{Au,max}$ and its corresponding value $d_{Sb,eff}$. Now we turn to the properties of the bilayers with $d_{Au} < d_{Au,max}$. As already mentioned the analysis of the UPS and XPS measurements on Sb/Au bilayers allows Boyen *et al* [6] to determine the average Au concentration of the amorphous interface as a function of d_{Au}; see figure 6 of reference [6]. With the knowledge of x as a function of d_{Au} we are able to compare $S/T|_{T\to 0}$ and ρ for the bilayers directly with the corresponding data obtained for three-dimensional amorphous Au_xSb_{100-x} alloys.

In contrast to measurements of transport properties, photoemission measurements allow us to determine local properties of alloys. In the insulating phase of the Sb/Au bilayers ($d_{Au} < d_{Au,min} = 0.11$ nm) a local Au concentration of $Au_{34}Sb_{66}$ was observed [6]. We believe that in the insulating phase of amorphous Au_xSb_{100-x} alloys as well as Sb/Au bilayers, atomic clusters of $AuSb_2$ are embedded in or on top of amorphous Sb. With increasing x or d_{Au} the clusters get closer and closer together. Finally at the percolation limit a continuous path is formed. Above this limit the shape of the Au 5d band and the shift of the Au 4f core levels change with x and d_{Au} in the same way.

Figure 6 shows the low-temperature slope of the thermoelectric power of the Sb/Au bilayers as a function of the Au content of their amorphous interfaces. For comparison corresponding data on the diffusion thermopower of the amorphous Au_xSb_{100-x} alloys are also shown. Additional contributions caused by virtual electron–phonon interactions which are responsible for the occurrence of the minimum in the range 14 at.% $< x <$ 40 at.% in figure 6 of reference [11] are subtracted. Details are given in [11].

Figure 7 shows the resistivity of the Sb/Au bilayers as a function of the Au content of the amorphous interfaces. In addition the values of ρ of amorphous Au_xSb_{100-x} alloys are shown also.

The last two figures have in common that the concentration dependences of the corresponding values are much more pronounced in the case of the Sb/Au bilayers than in the case of the amorphous Au_xSb_{100-x} alloys, while at high Au concentration the values start at about the same level. We propose that the quasi-two-dimensional character of the amorphous interface of the bilayers is responsible for this difference. Their thickness $d = d_{Au} + d_{Sb,eff}$ varies from $d = 2.8$ nm for the highest Au coverage ($x = 80$ at.%) to $d = 1.1$ nm for the lowest Au coverage ($x \approx 40$ at%) while the amorphous Au_xSb_{100-x} alloys had nearly the same thickness of about 100–400 nm. In a two-dimensional bilayer of $AuSb_2$ clusters on top of a Sb substrate the chance of finding a continuous path through it is reduced in comparison with that for a three-dimensional sample of $AuSb_2$ clusters

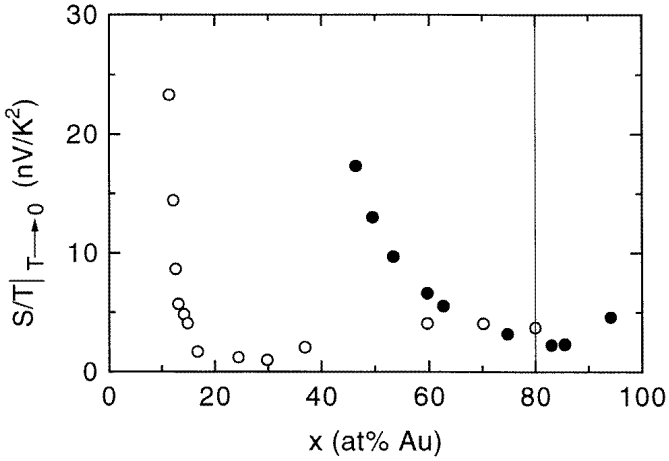

Figure 6. The low-temperature slope of the thermopower of Sb/Au bilayers (•) and of amorphous Au_xSb_{100-x} alloys (○) as functions of x. The vertical solid line marks the upper limit of the amorphous range of AuSb.

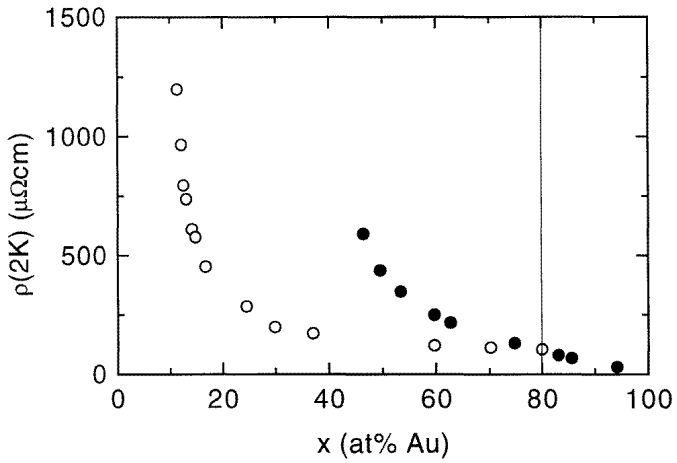

Figure 7. Electrical resistivities of Sb/Au bilayers (•) and of amorphous Au_xSb_{100-x} alloys (○) as functions of x. The vertical solid line marks the upper limit of the amorphous range of AuSb.

embedded in a Sb matrix.

The rapid increase of $R_\square(2\ \mathrm{K})$ at low d_{Au} and therefore $\rho(2\ \mathrm{K})$ at $x \approx 40$ at.% can be analysed in the framework of two-dimensional percolation theory as has been done for Ge/Bi and Ge/Pb ultrathin films [18] and Si/Nb sandwiches [19]. The analysis of our data which cover only a limited region gives values very similar to those given by the authors just mentioned. However, the percolation model ignores intermixing effects and chemical changes at the interface which are clearly manifested by UPS and XPS measurements [6]. In the case of three-dimensional amorphous Au_xSb_{100-x} alloys the metal–insulator transition in the metallic region was interpreted in terms of an Anderson transition [11]. Unfortunately in

the case of Sb/Au bilayers to less data in the metallic region next to $d_{\mathrm{Au,min}}$ were measured in the present investigation. In order to analyse the transition carefully more data for the region near the metal–insulator transition are needed.

5. Conclusions

Using measurements of the electrical resistance and the thermoelectric power of Sb/Au bilayers as functions of the thickness of the Au film, a behaviour was found which is very similar to that of amorphous Au_xSb_{100-x} alloys as a function of Au content. This similarity not only holds for the low-temperature data but also for the data obtained during annealing below the crystallization temperature. The pronounced increase of the low-temperature values of $R_\square$ and $S/T|_{T\to 0}$ at low Au coverages indicates a transition which is, in our opinion, caused by percolation and chemical interaction. The results of our investigation combined with those from photoemission measurements lead into the picture of the formation of an amorphous interface in Sb/Au bilayers as long as $d_{\mathrm{Au}} < 2$ nm. The thicknesses which characterize the amorphous interface are in the monolayer range and agree well with the values found in other investigations.

Acknowledgments

We thank H von Löhneysen, T Moser and M Sohn for valuable discussions. Financial support provided by the Deutsche Forschungsgemeinschaft in the initial stages of the investigation is gratefully acknowledged.

References

[1] Naugle D G 1967 *Phys. Lett.* **25A** 688
[2] Strongin M and Kammerer O F 1968 *J. Appl. Phys.* **39** 2509
[3] Strongin M, Thompson R S, Kammerer O F and Crow J E 1970 *Phys. Rev.* B **1** 1078
[4] Song S N, Li D X and Ketterson J B 1989 *J. Appl. Phys.* **66** 5360
[5] Nease B, Mack A M, Spalding G C, Martinez-Arizala G and Goldman A M 1994 *Physica* B **194–196** 2347
[6] Boyen H-G, Cossy-Favre A, Oelhafen P, Siber A, Ziemann P, Lauinger C, Moser T, Häussler P and Baumann F 1995 *Phys. Rev.* B **51** 1791
[7] Suhrmann R and Berndt W 1940 *Z. Phys.* **115** 17
[8] Richter H, Berckheimer H and Breitling G 1954 *Z. Naturf.* a **9** 236
[9] Hauser J J 1974 *Phys. Rev.* B **9** 2623
[10] Häussler P, Müller W H-G and Baumann F 1979 *Z. Phys.* B **35** 67
[11] Lauinger C and Baumann F 1995 *J. Phys.: Condens. Matter* **7** 1305
[12] Roberts R 1977 *Phil. Mag.* **36** 91
[13] Compans E 1989 *Rev. Sci. Instrum.* **60** 2715
[14] Trefny J U, Peters D S and Fox J N 1984 *J. Non-Cryst. Solids* **65** 215
[15] Sambles J R and Priest T W 1984 *J. Phys. F: Met. Phys.* **14** 1693
[16] Häussler P, Schneider M, Müller W H-G and Baumann F 1984 *Proc. 17th Int. Conf. on Low Temperature Physics* (Amsterdam: North-Holland)
[17] Boyen H-G, Cossy-Favre A, Gantner G, Stupp H, Lauinger C and Oelhafen P 1996 *J. Non-Cryst. Solids* at press
Boyen H-G 1995 *Habilitation* University of Basel
[18] Haviland D B, Liu Y and Goldman A M 1989 *Phys. Rev. Lett.* **62** 2180
[19] Song S N and Ketterson J B 1991 *Phys. Lett.* **155A** 325